RESPONSE OF SIMPLE, SCALE MODEL REACTOR VESSELS TO A SIMULATED HCDA LOADING*

D. J. CAGLIOSTRO, C. M. ROMANDER, A. L. FLORENCE

Poulter Laboratory, Stanford Research Institute, Menlo Park, California 94025, U.S.A.

SUMMARY

The safety of liquid metal fast breeder reactors (LMFBRs) depends in part on maintaining the reactor's primary containment (reactor vessel and primary cooling loops) during a hypothetical core disruptive accident (HCDA). To help evaluate the safety of LMFBRs, computer codes have been developed for predicting the structural response of LMFBRs to HCDAs. Validation of these codes is best done by performing experiments with simple scale models of a reactor.

The work described here was performed to verify modeling techniques used in two-dimensional axisymmetric fluid-structure-interaction codes. A well-defined energy source was applied in simple reactor models having well-defined material properties, dimensions with precision tolerances, and simple boundary conditions, and the loading, strain, and deformations were measured.

The experiments were performed in thick-walled and thin-walled vessels that are approximately 1/30-scale of the Clinch River Breeder Reactor (CRBR). The sodium coolant is simulated by water, and the HCDA load is simulated by the expansion of the detonation products of a low-density explosive detonated in the vessel core barrel. The detonation products expand from an initial pressure of 3700 psi down to 360 psi for a volume change of 410 cm^3, equal to the cover gas volume. The expansion produces 2.87 kW-sec of gas work up to slug impact on the vessel cover.

Piezoelectric quartz pressure transducers measure the loading pressure in the core and on the core support platform, the vessel wall, and the cover. Foil strain gages measure circumferential and axial strains on the vessel wall. The plastic work absorbed by the vessel before and after slug impact is calculated from the strain measurements and the post-test deformation profiles.

In the thick-walled vessel, the peak pressures are 3000 psi on the core support platform, 6000 psi on the vessel wall, and 14,000 psi on the cover. The cover pressure rapidly drops to 7000 psi corresponding to slug impact pressure.

In the thin-walled vessel, the platform and wall pressures are 50% lower and the cover pressure is only 7% lower. Peak circumferential wall strains occur 1-1/4 inches below the cover and are 3.5%. To slug impact, the vessel absorbs 0.44 kW-sec of plastic work and the slug gains 2.6 kW-sec of kinetic energy. After impact the vessel absorbs an additional 1.38 kW-sec of strain energy, about 53% of the slug kinetic energy. The effect of core barrel flexibility on the loads in a thin-walled vessel is negligible for the HCDA load simulated. The posttest deformations of the vessel with a rigid core are the same as those with a flexible core barrel in the upper half of the vessels, but are about twice as large in the lower half.

The results of these experiments are presented in a form suitable for verifying two-dimensional fluid-structure interaction codes designed to predict the response of reactor vessels to HCDA loads.

* This work was supported by Argonne National Laboratory, Argonne, Illinois 60439, under Contract No. 31-109-38-2655.

1. Introduction

The reactor vessel forms part of the primary containment of loop-type liquid metal fast breeder reactors (LMFBRs). As part of the safety analysis of LMFBRs, two-dimensional, fluid-structure-interaction codes have been developed to calculate the response of the reactor vessel to core disruptive accident (CDA) loads (for example, references[1] and [2]). This paper presents the results of experiments that provide data for validating the modeling techniques used in these codes. The experiments were conducted in simplified 1/30-scale models of a reactor vessel in which water simulated the liquid sodium coolant, and a low density explosive energy source in the vessel core barrel simulated a CDA load. The vessels do not model any particular reactor vessel; indeed, the vessel walls and core barrels are relatively thicker than, for example, those of the Clinch River Breeder Reactor. The energy source had been used to simulate a 150 MW-sec accident in 1/30- and 1/10-scale models of the Fast Test Reactor [3].

One thick-walled (rigid) vessel and two thin-walled (flexible) vessel experiments are described. We discuss the effects of vessel wall and core barrel flexibility on the loads in the vessels and their response to the simulated load. These effects would be greater in real reactors, which have relatively thinner walls and core barrels than the flexible models used here. We do not compare the experimental data with code predictions.

2. Description of Experiments

2.1 Rigid Vessel Experiment

The loading pressures in a vessel with only small elastic strains were measured in the thick-walled vessel shown in Figure 1. The vessel consisted of a steel cylinder sealed at the top and bottom by thick steel plates and a thick-walled (rigid) core barrel. We measured loading pressures in the core barrel, on the core-support platform, and on the vessel wall and cover.

2.2 Flexible Vessel Experiments

Two experiments were performed to investigate the effects of vessel wall and core barrel flexibility on the loading pressures in a thin-walled vessel and on its plastic response to these loads. The vessels, shown in Figure 2, had inside dimensions approximately equal to those of the rigid vessel. The cover and platform were clamped and bolted to thick steel plates that were connected to each other by steel studs to ensure simple boundary conditions--zero axial and radial displacement and zero rotation at the vessel ends. The vessel wall was made from annealed Ni 200 to approximately simulate at room temperature the stress-strain properties of 304 SS at reactor operating temperatures ($\sim$1000°F). The first experiment was performed with a one-inch-thick (rigid) steel core barrel, and the second with a 0.050-inch-thick (flexible) aluminum core barrel enclosing a 0.950-inch-thick lead liner. The stress-strain curves for the flexible vessel materials are shown in Figure 3.

In each experiment we measured the loading pressure on the core platform and vessel wall and cover at the same locations as in the rigid vessel, the circumferential wall strains, and the deformation profiles of the vessel wall. In the experiment with the rigid core barrel we measured the core pressure, and in the experiment with the flexible core barrel we measured the circumferential strain on the outside of the aluminum core barrel.

2.3 Instrumentation

Piezoelectric quartz pressure transducers with a resonant frequency of 450 kHz and a 1-μsec rise time were used to measure the loading pressures. High-elongation foil strain gages were used to measure the circumferential wall and core barrel strains. Based on six calibration and rigid vessel experiments [4], the loading pressures are reproducible within ±10% of the average. The accuracy of the strain measurements is about ±2%. The variation in the radial deflections at a given axial location is 3.6% of the average in areas of large deflections and 26% in areas of small deflections.

2.4 Energy Source

The energy source consisted of an 8-g charge of a low-density explosive (0.33 g/cm^3) in a vented steel canister that was bolted inside the empty core barrel. The low-density explosive was a mixture of powdered PETN* and hollow, glass spheres (Microballoons†), 65/35 by weight. The characteristics and calibration of the energy source have been described by Cagliostro et al. [5] and by Florence et al. [3].

Figure 4 shows the pressure- and gas work-volume change relationships for the energy source. The peak pressure in the lower core (226.5 cm^3) is about 255 bars (3700 psi) and the pressure decreases to about 25 bars (360 psi) as the detonation products expand to ΔV = 410 cm^3, the cover gas volume. The gas work expended by the detonation products in displacing the water pool into the cover gas region is 2.87 kW-sec. Based on the results of calibration experiments performed in the rigid vessel, the reproducibility of the energy source is estimated to be about ±5%.

3. Discussion of Results

3.1 Loading Pressures in the Rigid Vessel

After detonation of the charge, the pressure in the core, shown in Figure 5(a), increases to 3700 psi in about 125 μsec and decreases to about 360 psi in about 0.82 msec as the detonation products expand against the water and accelerate it upward into the cover.

The pressure on the platform, Figure 5(b), begins at about t = 0.18 msec, the time for pressure waves to reach the platform. The pressure reaches a peak and then decreases to zero as expansion waves reflected from the water surface arrive at the platform. At t = 1.0 msec the pressure wave caused by slug impact on the cover reaches the platform and increases the platform pressure to about 2600 psi.

The pressure on the vessel wall 6 inches above the platform, Figure 5(c), begins to increase to about 1500 psi at t = 0.1 msec. As expansion waves from the water surface pass by the gage and reflect from the platform and again pass by the gage, the wall pressure decreases to zero at t = 0.4 msec. At t = 0.85 msec the pressure wave caused by slug impact on the cover reaches the wall gage and increases the pressure there to about 6000 psi. The pressure then decreases as expansion waves from the bubble surface reach the wall. At t = 1.1 msec the impact pressure wave reflected from the platform reaches the pressure gage, increasing the pressure to 2500 psi.

The pressure on the vessel cover, Figures 5(d) and 5(e) is zero until t = 0.75 msec when the slug accelerated to 108 ft/sec impacts the cover. The pressure increases to about

---

*PETN ($C_5H_8O_{12}N_4$) pentaerythritol tetranitrate

†Manufactured by Emerson and Cummings, Inc., Canton, Massachusetts.

14,000 psi as the air in the cover gas region is compressed and the slug impacts the cover. The pressure drops sharply to about 7000 psi and remains at this pressure until the impact pressure wave travels from the cover to the gas bubble where it is reflected as an expansion wave and returns to the cover, decreasing the cover pressure to zero at t = 0.95 msec. The impact pressure corresponding to the planar impact of a water slug on a rigid wall at 108 ft/sec is 7080 psi. Neglecting comparison of the cover gas, this is in excellent agreement with the measured impact pressure.

3.2 Comparison of Loading Pressures in Rigid and Flexible Vessels

The pressure in the rigid core barrel, Figure 5(a), of each vessel is the same, showing that the deforming vessel wall has no effect on these loads.

The pressure on the platform, however, is significantly higher in the rigid vessel (3000 psi) than in the flexible vessel (1500 psi). This difference occurs because the expansion of the flexible vessel wall relieves the pressurized water between the core and the vessel wall. Similarly, the reflected impact pressure wave reaching the platform is much lower in the flexible vessel than in the rigid vessel because the pressure wave is attenuated by the expansion of the vessel wall near the cover.

The wall pressures 6 inches above the platform, Figure 5(c), differ significantly when the impact pressure wave arrives. Again, the much lower pressure in the flexible vessel is due to the attenuation of the impact pressure wave by the expanding wall.

Except for the relatively high sharp peak that occurs in compressing the cover gas in the rigid vessel, the peak load on the cover, Figures 5(d) and 5(e), is 7000 psi in the rigid vessel and 6500 psi in the flexible vessel. This 7% difference means that the impact velocity of the slug differs by only 7% and that the gas work gone into plastically deforming the vessel before impact is 14% of the gas work gone into the kinetic energy of the slug. (Indeed, the strain energy measurements, discussed below in Section 3.4, show that the strain energy absorbed by the flexible vessels before slug impact is 0.44 kW-sec, about 15% of the kinetic energy of the slug at impact in the rigid vessels.) The duration of the slug impact is much shorter in the flexible vessel than in the rigid vessel because the deforming wall near the cover generates expansion waves in the water that relieve the impact pressure sooner than those from the gas bubble.

3.3 Effects of Core Barrel Flexibility on Loading Pressures in Flexible Vessels

As shown in Figure 6, the flexible core barrel has little effect on the pressures in the flexible vessel. The only place a significant difference occurs is on the vessel platform where the loading begins about 150 μsec earlier and is slightly less than in the vessel with a rigid core. The loading occurs earlier because the platform pressure is transmitted to the platform by the expansion of the flexible core, which pressurizes the water between the core and the vessel wall before the pressure waves traveling out of the top of the core reach the platform. The magnitude of the loading is about 10% less in the vessel with a flexible core because of the energy loss in expanding the core and the presence of expansion waves caused by the wall expansion.

3.4 Effects of Core Barrel Flexibility on the Strain and Deformation in Flexible Vessels

As shown in Figure 7, core barrel flexibility affects the wall strains only near the core barrel. The strain histories in the upper half of the vessels, Figures 7(a), (b), and (c), are about the same in shape and magnitude, whereas the strain histories in the lower

half of the vessels, Figures 7(d) and (e), show two distinct response phases--the first before slug impact and the second after slug impact. Before slug impact, the vessel walls respond to the loads transmitted through the water by the expansion of the core barrel and by the high-pressure detonation products accelerating the water upward. After slug impact, the vessel walls respond to the slug impact pressure wave in the water. As the impact pressure wave moves down the vessel, it expands the vessel walls and attenuates. The attenuating pressure wave causes the decreasing magnitude of strains recorded at locations 1, 2, and 3, which are 3.4, 4.5, and 5.5 inches from the cover.

The effect of the flexible core barrel on the strain in the lower half of the vessel is shown in Figures 7(d) and (e). At location 4, which is 4 inches above the platform at the level of the top of the core, the wall strain in the vessel with a flexible core is about 10% less than in the vessel with a rigid core. At location 5 (2 inches above the vessel platform), the difference in vessel response is greater; the maximum strain in the vessel with a flexible core is about half of that in the vessel with a rigid core. Although these results were not expected, they are in line with the comparison of vessel loadings discussed earlier.

Figure 8 compares the vessel deformation profiles before and after slug impact. Before slug impact (t = 0.75 msec) deformations occur mainly in the vicinity of the core barrel and are about twice as large in the vessel with a rigid core barrel than in the vessel with a flexible core barrel. In the upper half of the vessel, the wall deformations are relatively small until after slug impact. Then they increase to a peak of about 140 mils (3.5% strain) at 1.25 inches below the cover with the deformations in both vessels the same. The deformations are the same in both vessels because the impact velocities in both vessels have been affected little by the differences in vessel strain energies absorbed before slug impact (0.44 kW-sec with the rigid core barrel and 0.45 kW-sec with the flexible core barrel).

The strain energies of both vessels and of the flexible core barrel as functions of time are shown in Figure 9 and tabulated in Table I. Before slug impact, the strain energy in the vessel with a rigid core barrel equals the strain energy in the vessel with a flexible core barrel. Therefore, the kinetic energy and thus the impact velocity of the slug in each vessel is practically the same. This results in the impact pressures on the cover being equal as shown in Figure 6 and in the final deformations near the cover being equal as shown in Figure 8.

4. Acknowledgments

We gratefully acknowledge the technical guidance of S. H. Fistedis and G. Nagumo of Argonne National Laboratory and A. L. Florence of Stanford Research Institute. At SRI, C. E. Blahnik designed the vessels, J. H. Busma coordinated their design and construction, and G. R. Greenfield helped ensure the successful performance of the experiments.

References

[1] CHANG, Y. W., GVILDYS, J., FISTEDIS, S. H., "Calculations of the Dynamic Response of the Primary Containment Using a Two-Dimensional Hydrodynamic-Elastic-Plastic Code," Trans. Am. Nucl. Soc. 15, p. 818 (1972).

[2] WANG, C. Y., CHU, H. Y., CHANG, Y. W., FISTEDIS, S. H., "Application of the Implicit Eulerian Method (ICECO) to Fast Reactor Containments," Proceedings Third Intl. Conference on Structural Mechanics in Reactor Technology, London, United Kingdom, September 1-5, 1975 Paper E 3/4.

[3] FLORENCE, A. L., ABRAHAMSON, G. R., CAGLIOSTRO, D. J., "Hypothetical Core Disruptive Accident Experiments on Simple Fast Test Reactor Models," Nucl. Eng. Design 38, pp. 95-108 (1976).

[4] CAGLIOSTRO, D. J., ROMANDER, C. M., "Experiments on the Response of Rigid and Flexible Reactor Vessel Models to a Simulated Hypothetical Core Disruptive Accident," Fifth Interim Report to Argonne National Laboratory on SRI Project PYD 1960 (1976).

[5] CAGLIOSTRO, D. J., FLORENCE, A. L., ABRAHAMSON, G. R., NAGUMO, G., "Characterization of an Energy Source for Modeling Hypothetical Core Disruptive Accidents in Nuclear Reactors," Nucl. Eng. Design 27 (1), pp. 94-105 (March 1974).

Table I

ENERGY PARTITIONING IN FLEXIBLE VESSEL EXPERIMENTS

	Energy (kW-sec)	
	FV 101, Rigid Core Barrel	FV 102, Flexible Core Barrel
Gas work at V_c^*	2.87	2.87
Gas work at $V_c + \Delta V_v^\dagger$	3.25	3.25
Strain energy at impact		
Vessel	0.44	0.28
Core	0.0	0.17
Slug energy at impact	2.6	2.59
Total strain energy		
Vessel	1.82	1.69
Core	0.00	0.17
Total	1.82	1.86

*V_c = cover gas volume.

†ΔV_v = volume change of vessel.

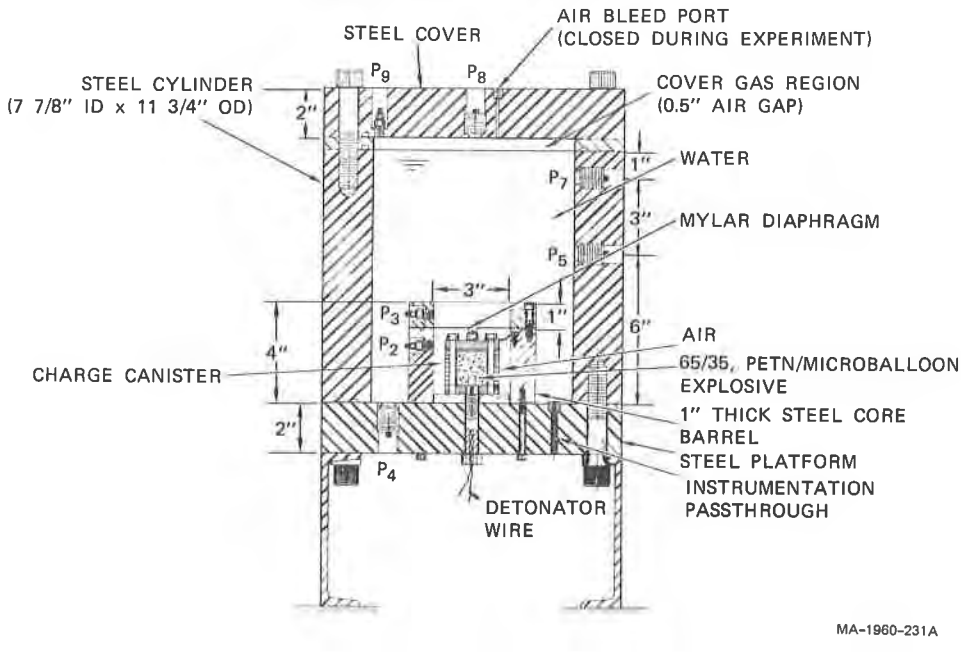

Figure 1. Rigid Vessel with Instrumentation

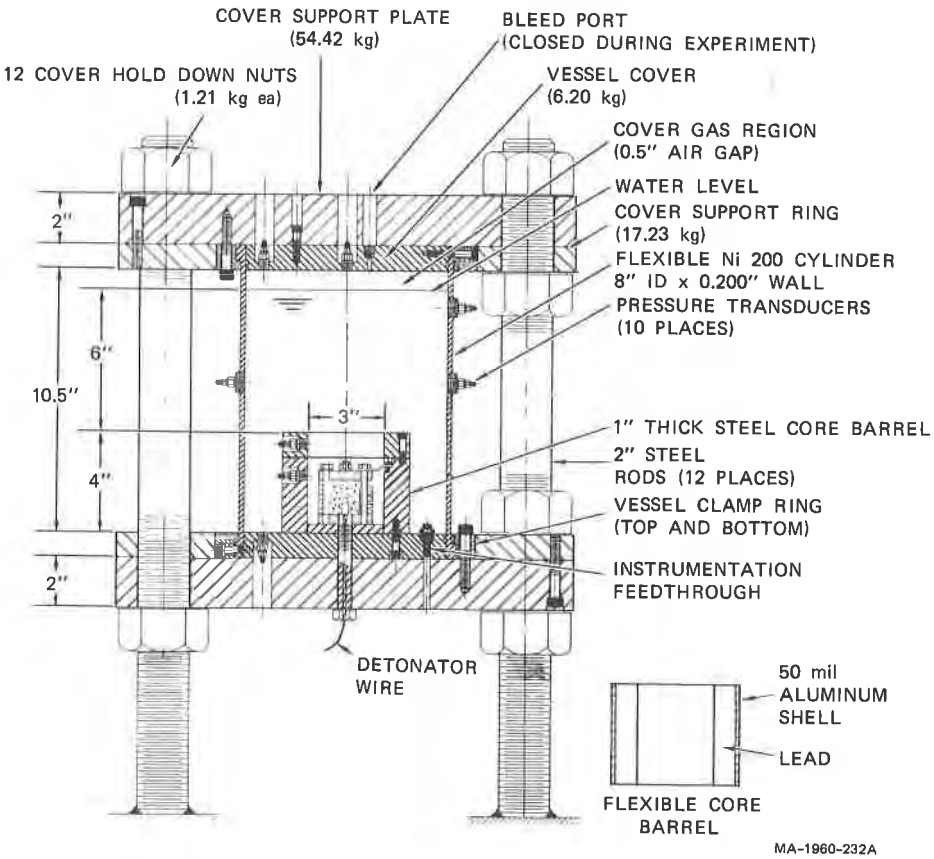

Figure 2. Flexible Vessel Assembly

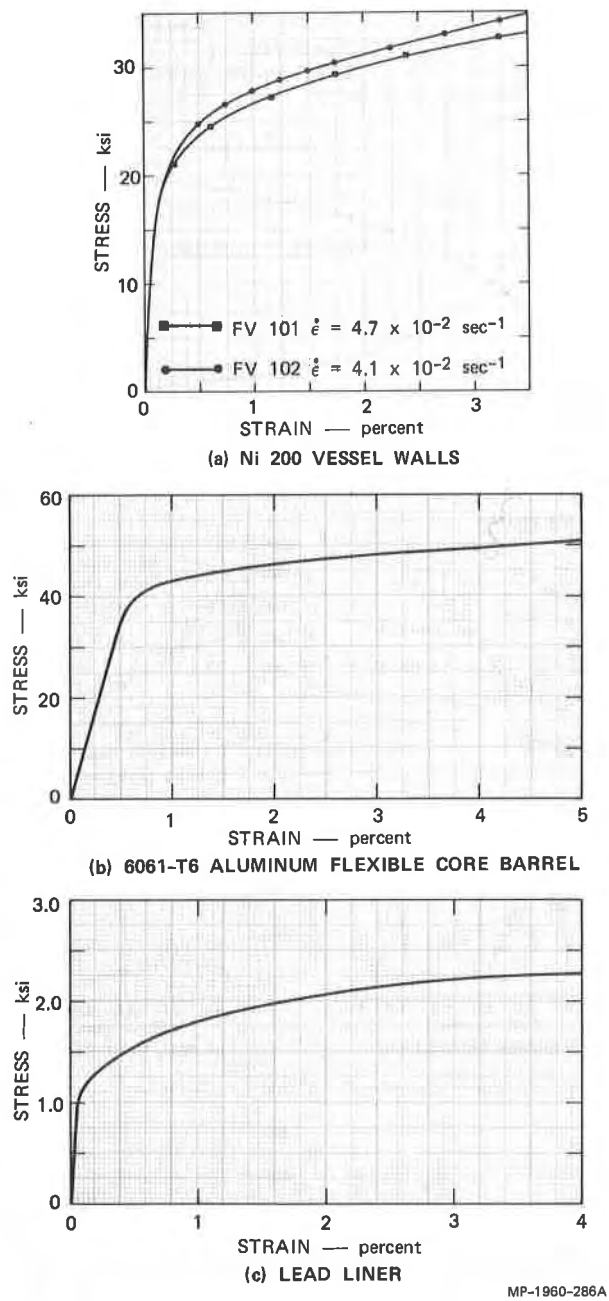

Figure 3. Stress-Strain Curves for Flexible Vessel Materials

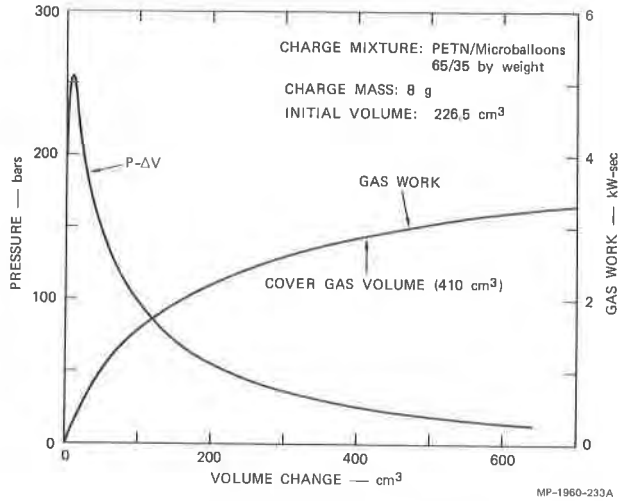

Figure 4. Pressure-and Gas Work-Volume Change Relationships for Energy Source

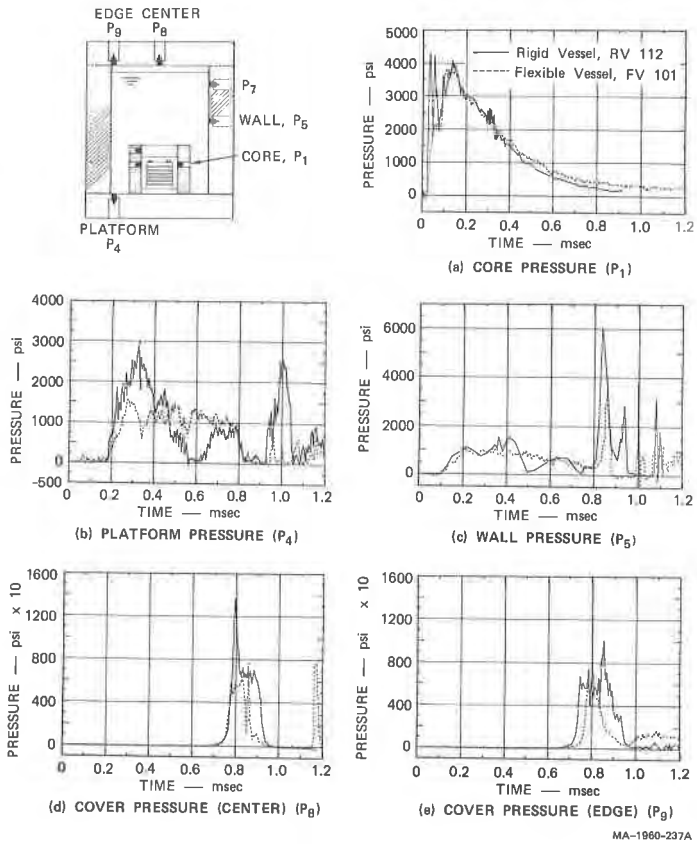

Figure 5. Loading Pressures in Rigid and Flexible Vessels with Rigid Core Barrels.

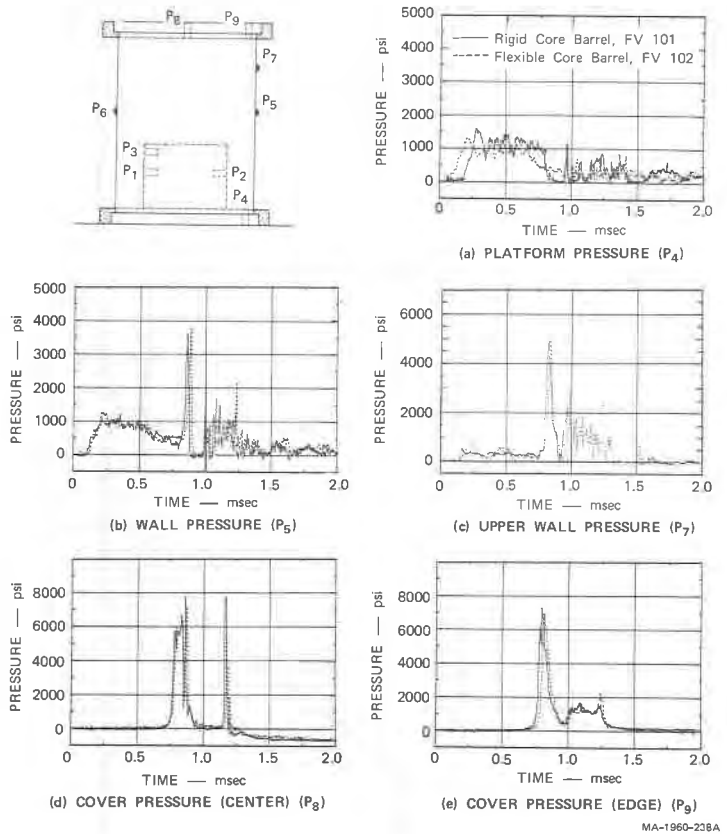

Figure 6. Effect of Core Barrel Flexibility on Loading Pressures in Flexible Vessels.

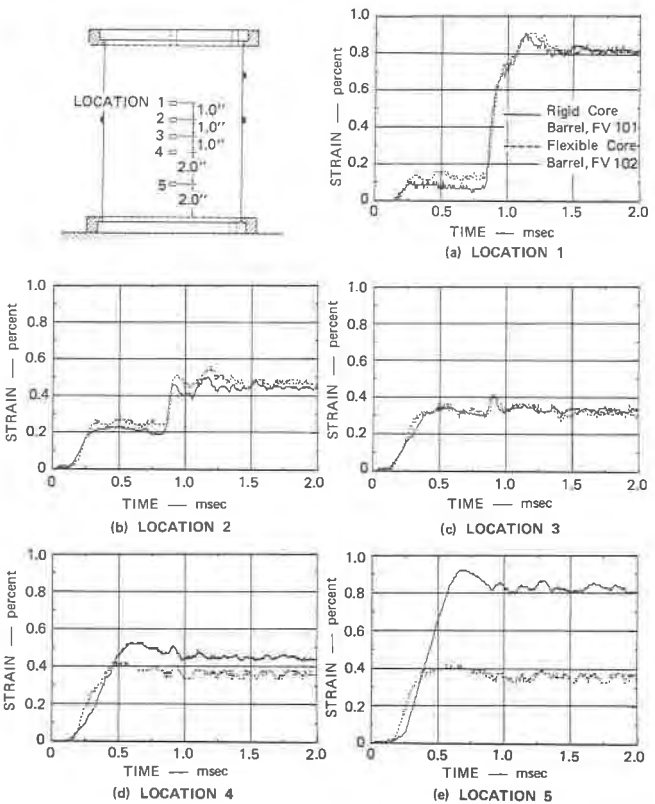

Figure 7. Effect of Core Barrel Flexibility on Strain-Time Response of Flexible Vessels

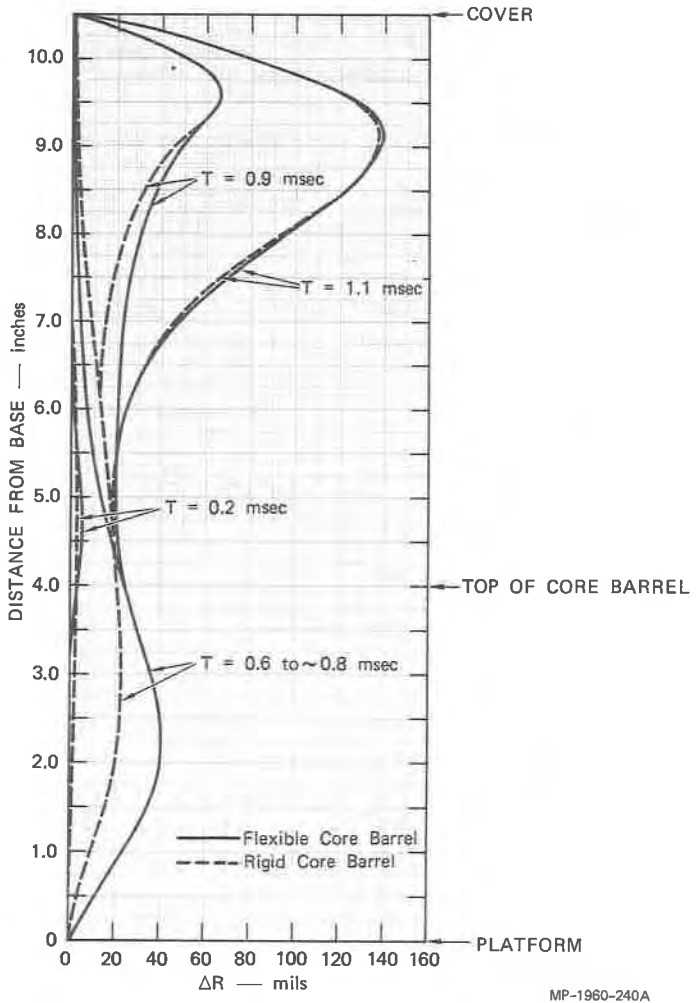

Figure 8. Effect of Core Barrel Flexibility on Deformation-Time Profiles of Flexible Vessels.

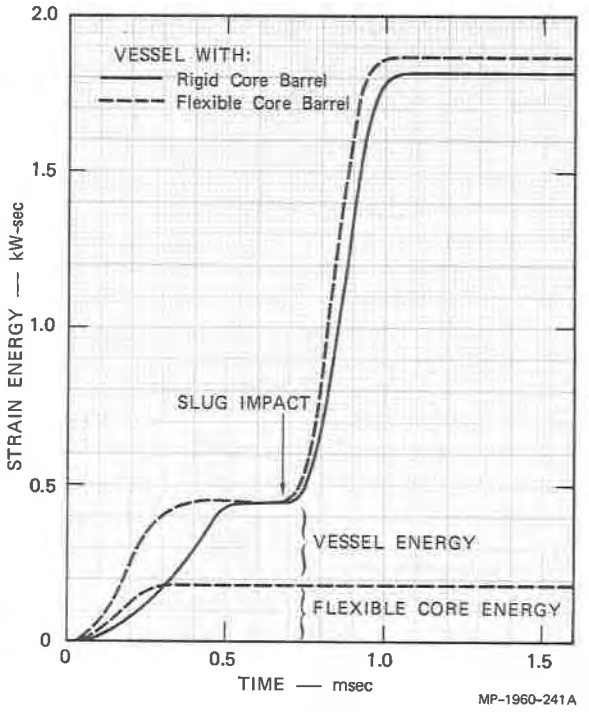

Figure 9. Effect of Core Barrel Flexibility on Strain Energy Absorbed During Flexible Vessel Experiments